

DESY 99-045
hep-ph/9904243
April 1999

Top Quark Physics*

Thomas Teubner

Deutsches Elektronen-Synchrotron DESY, D-22603 Hamburg, Germany

* Presented at the *Cracow Epiphany Conference on Electron-Positron Colliders*, 5-10 January 1999, Krakow, Poland.

Top Quark Physics*

THOMAS TEUBNER

Deutsches Elektronen-Synchrotron DESY, D-22607 Hamburg, Germany

In this contribution I review the physics of top quarks at a future Linear Collider. Main emphasis is put on the process $e^+e^- \rightarrow t\bar{t}$ close to threshold. Different physical observables, their sensitivity to the basic parameters and their theoretical prediction are discussed. Recent higher order calculations are shown to have a considerable impact on a precise determination of the top quark mass. It is pointed out how the use of mass definitions different from the pole mass scheme become important in this respect. Continuum top quark production above threshold is discussed briefly.

PACS numbers: 14.65.Ha, 13.90.+i, 12.38.Bx

1. Introduction

Top Quark Physics will be one of the main physics cases for future collider physics. Whereas the first direct discovery of top was one of the main successes of the proton collider at Fermilab, the precise measurement of the top quark mass and its couplings will remain the task of a future lepton collider.

But why should we be interested in such high precision measurements in the top sector? The top quark is the heaviest elementary particle observed up to now. Because of its very high mass $m_t \approx 175$ GeV it plays a prominent role for our understanding of the Standard Model (SM) and the physics beyond. Already before its direct observation there was indirect evidence of the large top quark mass: through radiative corrections m_t enters quadratically into the ρ parameter. From precision measurements of the electroweak parameters M_Z , M_W , $\sin^2 \theta_W$ and G_F a top quark mass was predicted in striking agreement with the value measured at Fermilab. Within the framework of the SM the mass of the Higgs boson can be constrained from the weak boson masses M_W and M_Z together with m_t : $M_H = f(M_Z, M_W, m_t)$. As the Higgs mass enters in logarithmic form, stringent mass bounds can

* Presented at the *Cracow Epiphany Conference on Electron-Positron Colliders*, 5-10 January 1999, Krakow, Poland.

be derived only once the other parameters are known with high accuracy. With an absolute uncertainty of the top quark mass $\Delta m_t \lesssim 200$ MeV the Higgs mass will be extracted with an accuracy better than 17%. This will constitute one of the strongest tests of the mechanism of electroweak symmetry breaking at the quantum level and therefore of our understanding of the structure of the SM.

At the starting time of a future Linear Collider (LC) Higgs boson(s) may hopefully already have been discovered with the hadron machine at Fermilab or at the LHC (assuming LEP2 is not the lucky one in the next future). Still, to pin down parameters precisely and to learn which sort of physics beyond the SM is realized in nature, many detailed studies will be required. With an expected accuracy of $\Delta m_t/m_t \approx 1 \cdot 10^{-3}$ ($\Delta m_b/m_b \simeq \mathcal{O}(\%)$) and the large Yukawa coupling $\lambda_t^2 \approx 0.5$ ($\lambda_b^2 \approx 4 \cdot 10^{-4}$) the top quark will play a key role in finding the theory that gives the link between masses and mixings and quarks and leptons.

Apart from that the large top quark mass has another important consequence: being much heavier than the W boson the top decays predominantly into the W and a bottom quark with the large (Born) decay rate

$$\Gamma_t^{(0)} = \frac{G_F m_t^3}{\sqrt{2} 8\pi} \approx 1.5 \text{ GeV} \gg \Lambda_{\text{QCD}}. \quad (1)$$

Therefore top is the only quark that lives too short to hadronize. The large width Γ_t serves as a welcome cut-off of non-perturbative effects [1] and the top quark behaves like a *free* quark. In this way top quark physics is an ideal test-laboratory for QCD at high scales, where predictions within perturbation theory are reliable.

Having these goals in mind a future e^+e^- Linear Collider (see e.g. [2, 3]) will be the ideal machine to study the top quark in detail. (The same will be true for a $\mu^+\mu^-$ collider, once technologically feasible.) The clean environment and generally small backgrounds make it complementary to hadron machines, where higher energies can be achieved more easily. In addition the collision of point-like, colourless leptons guarantees very good control of the systematic uncertainties. Operation with highly polarized electrons (and to a smaller extent also positrons) is realizable and will open new possibilities. Another option is the use of Compton back-scattered photons of intense lasers from the electron and positron bunches, allowing for operation of the e^+e^- collider in the $\gamma\gamma$ (or $e\gamma$) mode. These modes can be very useful for certain studies of the Higgs sector and other areas of electroweak physics, but will be less important for top quark physics. Therefore the following discussion will be limited to e^+e^- collisions.¹

¹ Reader interested in the physics of $\gamma\gamma$ collisions are referred to [2] (and references therein) for a general discussion and to [4] especially for $\gamma\gamma \rightarrow t\bar{t}$ at threshold.

The article is organized as follows: In Section 2 the scenario of top quark pair production at threshold is described in some detail. I discuss the important parameters, accessible observables and their sensitivity, and the corresponding theoretical predictions. Recent higher order calculations are reviewed. It will be shown how the large theoretical uncertainties in the shape of the cross section near threshold can be avoided by using a mass definition different from the pole mass scheme. In Section 3 a brief discussion of some important issues in top quark production above threshold is given. Section 4 contains the conclusions. For a comprehensive review of top quark physics (including top at hadron colliders) see also [5]. Clearly the rich field of top quark physics cannot be completely covered in this contribution, which is somewhat biased towards $t\bar{t}$ at threshold. This is also partly due to the author's experience. I would like to apologize to those who miss important information or feel own contributions to top physics not covered properly or not mentioned at all.

2. The $t\bar{t}$ Threshold

2.1. What's so special about the top threshold?

Close to the nominal production threshold $\sqrt{s} = 2m_t$ top and anti-top are produced with non-relativistic velocities $v = \sqrt{1 - 4m_t^2/s} \ll 1$. The exchange of (multiple, ladder-like) Coulombic gluons leads to a strong attractive interaction, proportional to $(\alpha_s/v)^n$. These terms are not suppressed and the usual expansion in α_s breaks down. Summation leads to the well known Coulomb enhancement factor at threshold, giving a smooth transition to the regime of bound state formation below threshold, which cannot be described using ordinary perturbation theory. In principle we would expect a picture like this with “Toponium” resonances similar to the case of bottom quarks which form the $\Upsilon(nS)$ mesons at threshold. However, in the case of top quarks, the rapid decay makes a formation of real $t\bar{t}$ bound states impossible. The width of the $t\bar{t}$ system is saturated by the decay of its constituents: $\Gamma_{t-\bar{t}} \approx 2\Gamma_t \approx 3 \text{ GeV}$. This is much larger than the expected level spacing and leads to a smearing of any sharp resonance structure, leaving only a remnant of the $1S$ peak visible in the excitation curve. Therefore there will be nothing like $t\bar{t}$ -spectroscopy to study at the top threshold. Nevertheless the short life-time of the top quarks also has a remarkable advantage: non-perturbative effects, hadronization and real (soft) gluon emission are suppressed by Γ_t , m_t .² Therefore, in contrast to

² For studies concerning the effects of real gluon emission see also Ref. [6].

the bottom (let alone the charm) quark sector, top quark production becomes calculable in perturbative QCD [7]. $t\bar{t}$ is, from the theoretical point of view, much “cleaner” than $c\bar{c}$ and $b\bar{b}$ and will allow for more detailed tests of the underlying theory and a more precise determination of the basic parameters m_t , α_s (and Γ_t). In this sense $t\bar{t}$ at threshold is a unique system, which deserves to be studied in detail at a future e^+e^- collider.

2.2. Parameters to be determined

- As mentioned already above the main goal will be a precise measurement of the top quark mass. Current analyses from CDF and D0 at the Tevatron at Fermilab determine m_t by reconstructing the mass event by event. Current values are

$$\begin{aligned} m_t^{\text{pole}} &= 176.0 \pm 6.5 \text{ GeV} && (\text{CDF [8]}), \\ m_t^{\text{pole}} &= 172.1 \pm 7.1 \text{ GeV} && (\text{D0 [9]}). \end{aligned} \quad (2)$$

The Run II at the Tevatron is expected to improve the accuracy down to maybe $\Delta m_t = 2 \text{ GeV}$. It looks impossible to reach a higher accuracy at hadron colliders. In contrast, with a threshold scan of the cross section at a future e^+e^- Linear Collider one will be able to reach $\Delta m_t = 200 \text{ MeV}$ or even better [3, 10, 11]. High luminosity will allow for very small statistical errors so that the accuracy will be limited mainly by systematic errors and theoretical uncertainties.

- The strong coupling α_s governs the interaction of t and \bar{t} . It enters the Coulombic potential $V(r) = -C_F \alpha_s / r$ which dominates close to threshold, as well as other corrections which get important at higher orders of perturbation theory (see below). α_s may either be taken as an input (with some error) measured independently at other experiments or, alternatively, can be determined simultaneously with m_t in a combined fit.

- The (free) top quark width Γ_t leads to the smearing of the resonances and strongly influences the shape of the cross section at threshold. As will be discussed below, Γ_t can be measured with good precision near threshold either in the $t\bar{t}$ production process or by help of observables specific to the decay.³ In the framework of the SM Γ_t can be predicted reliably: the first order α_s [13] and electroweak [14] corrections are known for some time (see also [15]), and recently even corrections of order α_s^2 became available [16]. The $\mathcal{O}(\alpha_s)$ corrections lower the Born result by about 10%, whereas $\mathcal{O}(\alpha_s^2)$ and electroweak contributions effectively cancel each other, with corrections

³ For a detailed discussion of top quark decays see also [12].

of about -2% and $+2\%$, respectively. In extensions of the SM the top quark decay rate can be significantly different from the SM value: new channels like the decay in a charged Higgs ($t \rightarrow bH^+$) in supersymmetric theories will lead to an increase of Γ_t . In models with a forth generation the Cabibbo-Kobayashi-Maskawa (CKM) quark-mixing-matrix element V_{tb} will be smaller than the SM value $V_{tb}^{(\text{SM})} \simeq 1$ and lead to a suppression of $\Gamma_t^{(\text{SM})}$.

- The electroweak couplings of the top quark enter both in production and decay. Especially in angular distributions (of the decay products) and in observables sensitive to the polarization of the top quarks deviations from the SM may be found. In principle even the influence of the Higgs on the $t\bar{t}$ production vertex should be visible [17]. Unfortunately, for the currently allowed range of Higgs-masses, effects due to (heavy) Higgs exchange mainly result in a “hard” vertex correction which changes the overall normalization of the cross section. As will be discussed below, contributions of this sort are in competition with uncertainties from other higher order corrections and therefore difficult to disentangle at the $t\bar{t}$ threshold.

Therefore, to determine the parameters with high precision and to eventually become sensitive to new physics, a thorough understanding of the SM physics, in particular the QCD dynamics, is mandatory.

2.3. Theory's tools to make predictions

How to predict the cross section close to threshold? In principle one could write the cross section as a sum over many overlapping resonances [18]:

$$\sigma(e^+e^- \rightarrow t\bar{t}) \sim -\text{Im} \sum_n \frac{|\psi_n(r=0)|^2}{E - E_n + i\Gamma_t}, \quad (3)$$

where ψ_n are the wave functions of the nS states with the corresponding Eigenenergies E_n . (Close to threshold S wave production is dominating with the contributions from P waves being suppressed by two powers of the velocity v . With $v \approx \alpha_s$ these contributions have to be considered only at next-to-next-to-leading order.) However, this explicit summation is not very convenient, as the sum does not converge fast, especially for positive energies $E = \sqrt{s} - 2m_t$. As shown by Fadin and Khoze [7], the problem can be solved within the formalism of non-relativistic Green functions:

$$\sigma(e^+e^- \rightarrow t\bar{t}) \sim -\text{Im} G(r=0, E + i\Gamma_t). \quad (4)$$

The Green function G is the solution of the Schrödinger equation

$$\left[\left(-\frac{\vec{\nabla}^2}{m_t} + V(\vec{r}) \right) - (E + i\Gamma_t) \right] G(\vec{r}, E + i\Gamma_t) = \delta^{(3)}(\vec{r}) \quad (5)$$

or, equivalently, the Lippmann-Schwinger equation in momentum space

$$\tilde{G}(\vec{p}, E + i\Gamma_t) = \tilde{G}_0 + \tilde{G}_0 \int \frac{d^3q}{(2\pi)^3} \tilde{V}(\vec{p} - \vec{q}) \tilde{G}(\vec{q}, E + i\Gamma_t), \quad (6)$$

where $\tilde{G}_0 \equiv (E + i\Gamma_t - p^2/m_t)^{-1}$ is the free Green function. At leading and next-to-leading order the continuation of the energy in the complex plane $E + i\Gamma_t$ is all that is needed to take care of the finite decay width of the top quarks. These equations can be solved numerically using a realistic QCD potential $V(r) = -C_F\alpha_s(r)/r$ or $\tilde{V}(q^2) = -4\pi C_F\alpha_s(q^2)/q^2$ to give the total cross section [19, 20, 21]

$$\sigma(e^+e^- \rightarrow \gamma^* \rightarrow t\bar{t}) = \frac{32\pi^2\alpha^2}{3m_t^2s} \text{Im} G(r=0, E + i\Gamma_t). \quad (7)$$

The top quark momentum distribution (differential with respect to the modulus of the top quark three momentum p), which reflects the Fermi motion in the would-be bound state and the instability of the top quarks, is obtained by

$$\frac{d\sigma(p, E + i\Gamma_t)}{dp} = \frac{16\alpha^2}{3sm_t^2} \Gamma_t p^2 \left| \tilde{G}(p, E + i\Gamma_t) \right|^2. \quad (8)$$

Eqs. (7, 8) are correct at leading order in α_s , v . At next-to-leading order (NLO) various new effects have to be taken into account. Apart from the well known $\mathcal{O}(\alpha_s)$ corrections to the static QCD potential [22] the exchange of “hard” gluons results in the vertex correction factor $(1 - 16\alpha_s/(3\pi))$ in the (total and differential) cross section [23]. Interference of the production through a virtual photon and a virtual Z boson leads to the interference of the vector current induced S wave with the axial-vector current induced P wave contributions. This S - P wave interference is suppressed by order v and drops out in the total cross section after the angular ($\cos\theta$) integration. However, it contributes to the differential rate and will be measured in observables like the forward-backward asymmetry \mathcal{A}_{FB} [24, 25]. In addition, at order α_s , there are final state corrections coming from gluon exchange between the produced t and \bar{t} and their strong interacting decay products b and \bar{b} . The final state interactions in the $t\bar{b}$ and $\bar{t}b$ systems factorize and are easily taken into account by using the (order α_s) corrected free top quark width Γ_t , with no other corrections at $\mathcal{O}(\alpha_s)$ [26, 27]. However, the

“crosstalk” between $t \bar{b}$, $\bar{t} b$ and $b \bar{b}$ leads to non-factorizable corrections which have to be considered in addition.⁴ These corrections are suppressed in the total cross section [28, 29], but contribute in differential distributions and hence in \mathcal{A}_{FB} .⁵ Results obtained in the framework of the non-relativistic Green function approach are available at $\mathcal{O}(\alpha_s)$, see [31, 32]. At the same accuracy polarization of the produced t and \bar{t} , depending on the polarization of the e^+ and e^- beams, has been studied in [25, 31, 32]. Therefore, at order (α_s, v) , theoretical predictions are available for a variety of observables at the top quark threshold, as will be discussed in the next paragraph.

Electroweak corrections to the $t\bar{t}$ production vertex have been calculated for the threshold region [33] as well as for general energies [34] in the SM and even in the Minimal Supersymmetric SM (MSSM), see [35].

2.4. Observables and their sensitivity

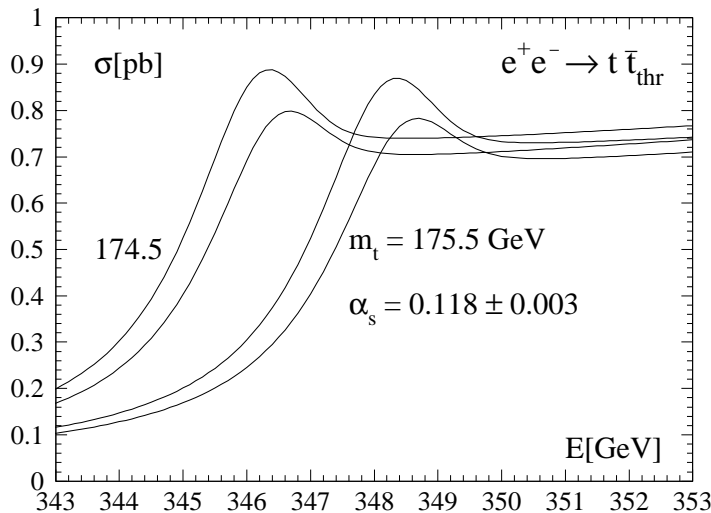


Fig. 1. Total cross section $\sigma(e^+e^- \rightarrow t\bar{t})$ (in pb) as a function of the total centre of mass energy for two different values of m_t and α_s . The upper curves correspond to $\alpha_s(M_Z) = 0.121$, the lower ones to $\alpha_s(M_Z) = 0.115$. (Figure taken from [3].)

- The (from the theoretical as well as from the experimental point of view) cleanest observable is the total cross section σ_{tot} . Depending on the

⁴ In principle hadronically decaying W bosons also take part in these final state interactions.

⁵ See also Ref. [30] and references therein for a discussion of the possible impact of colour reconnection effects on the top quark mass determination.

decays of the W^+ and W^- from the t and the \bar{t} quarks, $t\bar{t}$ decays into six jets (46%), four jets + $l + \nu_l$ (44%) or two jets + $ll' \nu \nu'$ (10%) (60, 35 and 5%, respectively, if $l = e, \mu$ only and τ -leptons are excluded). The main backgrounds are from $e^+e^- \rightarrow W^+W^-$, Z^0Z^0 and $f\bar{f}$ (plus gluons and photons). These processes are well under control as distinguishable from the signal (e.g. by higher Thrust or less jets) and constitute no big problem for the experimental analysis. The total cross section is mainly sensitive to m_t and α_s . Fig. 1 shows the cross section for two different values of the top quark mass and two values of the strong coupling, plotted over the total centre of mass energy. Note the correlation between m_t and α_s : higher top-masses lead to a shift of the remainder of the $1S$ peak to larger energies. In a similar way an increase of α_s is equivalent to a stronger potential (a larger negative binding energy) and hence lowers the peak position. I will come back to this point later. In practice, the shape of the cross section will not look as pronounced as in Fig. 1. Initial state radiation (of photons

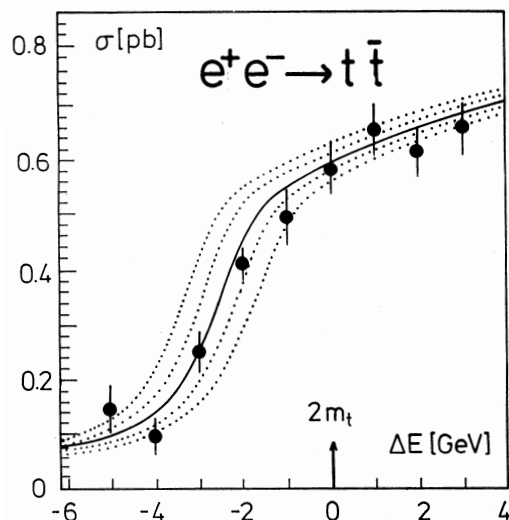


Fig. 2. Total cross section in the threshold region including initial-state and beamstrahlung. The errors of the data points correspond to an integrated luminosity of $\int \mathcal{L} = 50 \text{ fb}^{-1}$ in total. The dotted curves indicate shifts of the top mass by 200 and 400 MeV. (Figure taken from [3].)

from the e^+ and e^- beams) as well as the beamstrahlung-effects from the interaction of the e^+ and e^- bunches lead to a distortion of the original shape. Fig. 2 displays how the total cross section is expected to look under realistic conditions. The dots in the plot are Monte-Carlo generated “data points” of a typical planned threshold scan.

In addition σ_{tot} also depends on the Higgs mass M_H and the top quark

width Γ_t . As mentioned already above, the Higgs mainly influences the normalization of the cross section which will probably not allow for a high sensitivity to M_H once other uncertainties are taken into account. Γ_t , on the other hand, influences the shape: the smaller the width the more pronounced the peak. This will be used together with the sensitivity of other observables to measure Γ_t .

- Another observable is the momentum distribution $d\sigma/dp$, obtained from the reconstruction of the three momentum of the top (and antitop) quark. With the possible high statistics at a future Linear Collider the distribution can be well measured. As shown in Fig. 3, the peak position strongly depends on m_t but less on the QCD coupling: for higher values of m_t the distribution is peaked at much lower momenta, whereas the coupling strength mainly changes the normalization. Therefore a measurement of the

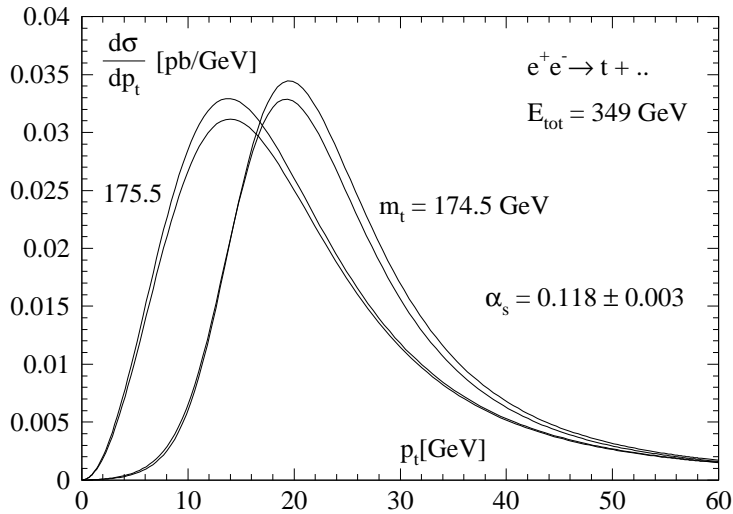


Fig. 3. The differential cross section $d\sigma/dp$ as a function of the top quark momentum p for a fixed value of the centre of mass energy (349 GeV). m_t and α_s are chosen as indicated. (Figure taken from [3].)

momentum distribution can help to disentangle the strong correlation of m_t and α_s in the total cross section (see [10]). There is also a less pronounced dependence on Γ_t .

- As mentioned above, S - P wave interference leads to a nontrivial $\cos \theta$ (θ being the angle between the e^- beam and the t direction) dependence of

the cross section. The resulting forward-backward asymmetry

$$\mathcal{A}_{\text{FB}} = \frac{1}{\sigma_{\text{tot}}} \left[\int_0^1 d \cos \theta - \int_{-1}^0 d \cos \theta \right] \frac{d\sigma}{d \cos \theta} \quad (9)$$

shows a considerable dependence on Γ_t and α_s , but is not very sensitive to m_t . In Fig. 4 \mathcal{A}_{FB} is plotted as a function of \sqrt{s} for three different

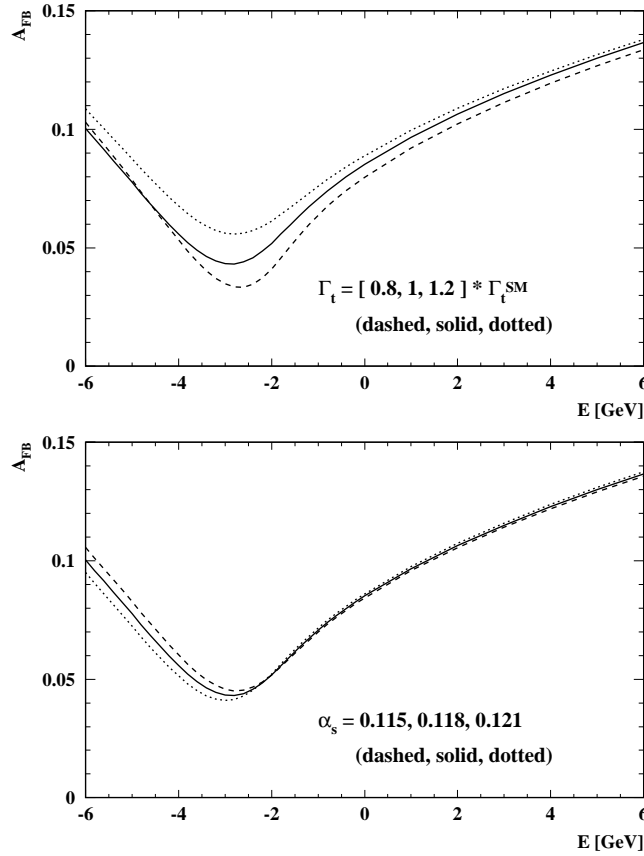


Fig. 4. Forward-backward asymmetry \mathcal{A}_{FB} as a function of $E = \sqrt{s} - 2m_t$ for three different values of the top quark width and the strong coupling. Upper plot: variation of Γ_t by $\pm 20\%$ around the SM value $\Gamma_t^{\text{SM}} = 1.43$ GeV and $\alpha_s(M_Z) = 0.118$. Lower plot: $\alpha_s(M_Z) = 0.115, 0.118, 0.121$ and $\Gamma_t = 1.43$ GeV. ($m_t = 175$ GeV.)

choices of Γ_t and α_s . With increasing width the overlap of S and P waves becomes bigger and hence the asymmetry is enhanced. Together with the total and differential cross section the measurement of \mathcal{A}_{FB} can be used to

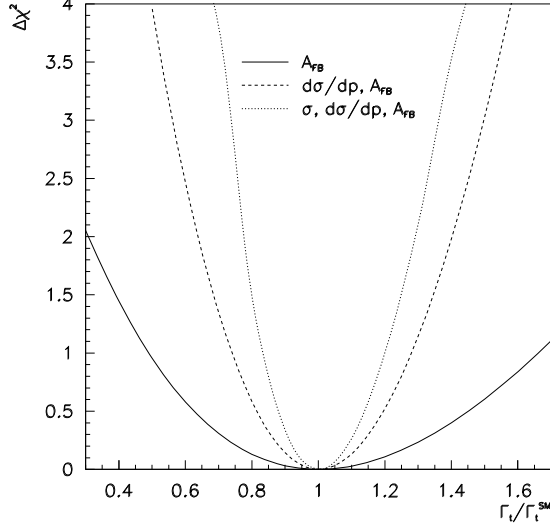


Fig. 5. Increase of the χ^2 of the fit as a function of the top quark width using the forward-backward asymmetry \mathcal{A}_{FB} (solid line), adding the top quark momentum distribution (dashed line) and the total cross section (dotted line). (Figure taken from [10].)

determine Γ_t by a fit. The sensitivity of such a fit to the different observables is demonstrated in Fig. 5.

Please note that the figures for the cross section and the asymmetry do not contain the (nonfactorizable) $\mathcal{O}(\alpha_s)$ rescattering corrections discussed in Section 2.3. They are absent in the total cross section but slightly change $d\sigma/dp$ and \mathcal{A}_{FB} , see [31, 32] for a detailed discussion.

- **Top Quark Polarization:** Near threshold S wave production dominates ($\vec{L} = 0$) and the total spin consists of the spins of the top and antitop quarks, $\vec{J}_{\gamma^*, Z^*} = \vec{S}_t + \vec{S}_{\bar{t}}$. In leading order the top spin is aligned with the e^+e^- beam direction. Even without polarization of the initial e^+ and e^- beams, the top quarks are produced with -40% (longitudinal) polarization. For a realistic (longitudinal) e^- polarization of $P_{e^-} = +80\%$ (-80%) and an unpolarized e^+ beam ($P_{e^+} = 0$) the top polarization amounts to $+60\%$ (-90%). This picture is changed only slightly due to S - P wave interference effects of $\mathcal{O}(v)$ and rescattering effects of $\mathcal{O}(\alpha_s)$, which lead to top polarizations perpendicular to the beam direction (transverse) and normal to the production plane. Normal polarization could also be induced by time reversal odd components of the $\gamma t\bar{t}$ - or $Z t\bar{t}$ -couplings, e.g. by an electric dipole

moment, signalling physics beyond the SM.

The influence of the bound state dynamics near threshold was calculated in the Green function formalism, including the polarization of the initial beams, the S - P wave interference contributions and the $\mathcal{O}(\alpha_s)$ rescattering effects [25, 31, 32]. Neglecting contributions due to rescattering, the three polarizations can be written as

$$\begin{aligned} |\vec{S}_{\parallel}| &= C_{\parallel}^0 + C_{\parallel}^1 \varphi_R(p, E) \cos \theta, \\ |\vec{S}_{\perp}| &= C_{\perp} \varphi_R(p, E) \sin \theta, \\ |\vec{S}_N| &= C_N \varphi_I(p, E) \sin \theta. \end{aligned} \quad (10)$$

The functions $\varphi_{R,I}$ contain all information about the threshold dynamics, whereas the coefficients C are dependent on the electroweak couplings and the e^+e^- polarization (see e.g. Ref. [31] for complete formulae). Fig. 6

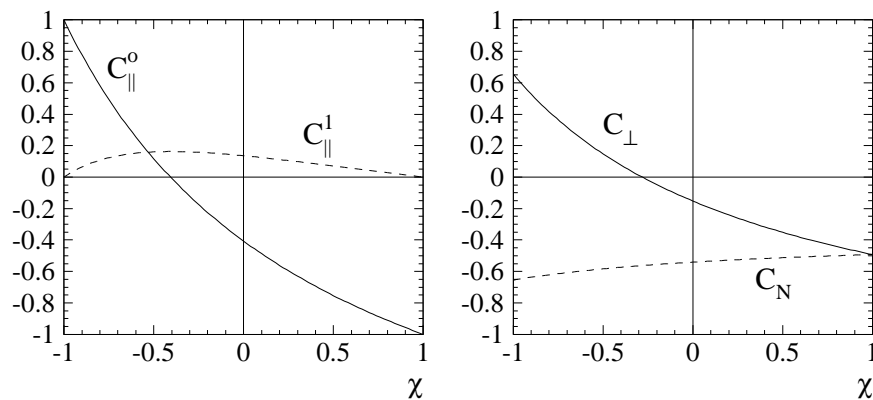


Fig. 6. Coefficients C as functions of the polarization χ as described in the text, for $\sqrt{s} = 180$ GeV and $\sin^2 \theta_W = 0.2317$.

shows the coefficients C_{\parallel}^0 , C_{\perp}^0 , C_{\perp} and C_N as functions of the effective polarization $\chi = (P_{e^+} - P_{e^-})/(1 - P_{e^+}P_{e^-})$. From Fig. 6 it becomes clear that by choosing the appropriate longitudinal polarization of the e^- beam one can tune the normal polarization of the top quarks \vec{S}_N to dominate. The functions $\varphi_{R,I}(p, E)$ are displayed in Fig. 7 for four different energies E around the threshold. Also shown is the result for free quarks, $\varphi_R = p/m_t$.

The normal polarization depends basically on the parameters Γ_t , α_s and is relatively stable against rescattering corrections. The α_s dependence can be understood from the case of stable quarks and a pure Coulomb potential, where the analytical solution exists [36]: $\varphi_I \rightarrow \frac{2}{3} \alpha_s$. In contrast, the sub-leading (angular dependent) part of the longitudinal polarization and the

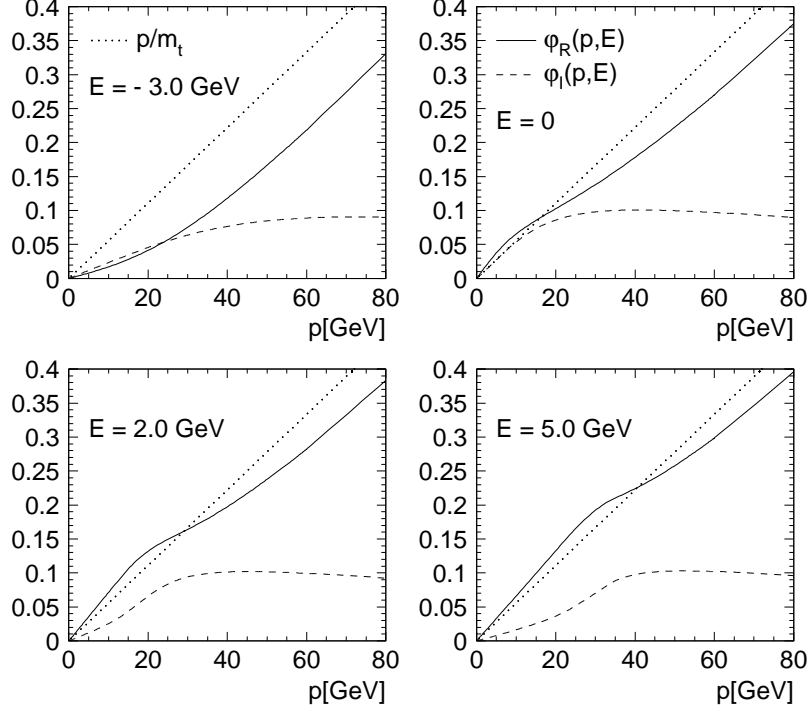


Fig. 7. Functions $\varphi_R(p, E)$ (solid curves) and $\varphi_I(p, E)$ (dashed) for four different energies close to threshold ($m_t = 180$ GeV, $\alpha_s = 0.125$). The dotted lines show the free particle result $\varphi_R = p/m_t$. (Figure taken from [31].)

transverse polarization both are (strongly) changed by rescattering corrections, but vanish after angular integration. For a detailed discussion of the rescattering corrections and the construction of inclusive and exclusive observables which are sensitive to the top quark polarization, see [31, 32, 37]. Let me just note here that the rescattering corrections destroy the factorization of the production and decay of the polarized top quarks. Nevertheless, observables can be constructed which depend neither on the subtleties of the $t\bar{t}$ production process nor on rescattering corrections, but only on the decay of free polarized quarks, even in the presence of anomalous top-decay vertices (see [32, 38]).

- Axial contributions to the angular integrated cross section: P wave contributions arise not only at $\mathcal{O}(v)$ due to S - P wave interference but also as P^2 -terms at next-to-next-to-leading order (NNLO). These contributions are suppressed by v^2 close to threshold. Still, they contribute at the percent level and have to be taken into account at the NNLO-accuracy discussed

below. In addition these axial current induced corrections are an independent observable and strongly depend on the polarization of the e^+e^- beams. Numerical results for the total and differential cross section were obtained recently within the formalism of non-relativistic Green functions [39]. Fig. 8 shows the total cross section as a function of the energy with and without these contributions and their size relative to the pure S wave result for three different values of the e^- polarization. A cut-off $p_{\max} = m_t/2$ has been applied to cure the divergence of the integrated P wave Green function coming from the large momentum region, where the non-relativistic approximation breaks down.

2.5. Large next-to-next-to-leading order corrections

In view of the size of the NLO corrections one may ask how accurate the theoretical predictions are. To answer this question within perturbation theory convincingly one has to go to the next order, in our case to the NNLO. The first step in this direction was done by M. Peter who calculated the $\mathcal{O}(\alpha_s^2)$ corrections to the static potential [40]. They turned out to be sizeable and, furthermore, indicate limitations of the accuracy achievable due to the asymptoticness of the perturbative series. As was studied in [41], the series for the effective coupling in the Coulomb potential behaves differently in the position and in the momentum space. Although potentials formally may differ only in N³LO, the resulting theoretical uncertainty of the total cross section in the $1S$ peak region is estimated to be of the order 6% [41].

Recently results of the complete NNLO relativistic corrections⁶ to $t\bar{t}$ production near threshold became available [42, 43, 44, 45]. The results are in fair agreement and modify the NLO prediction considerably. In the following I will briefly describe the calculation and results.

Calculation and results. The problem can be formulated most transparently in the framework of effective field theories. There one makes use of the strong hierarchy of the physical scales top mass, momentum, kinetic energy and Λ_{QCD} with $m_t \gg m_tv \gg m_tv^2 \gg \Lambda_{\text{QCD}}$ by integrating out “hard” gluons with momenta large compared to the scales relevant for the nonrelativistic $t\bar{t}$ dynamics. This leads to non-relativistic QCD (NRQCD) [46]. With $m_tv \gg \Lambda_{\text{QCD}}$ one can go one step further and integrate out gluonic (and light quark) momenta of order m_tv . Doing so one arrives at

⁶ Here NNLO means corrections of the order $\mathcal{O}(\alpha_s^2, \alpha_sv, v^2)$ relative to the Born result which contains the resummation of the leading $(\alpha_s/v)^n$ terms.

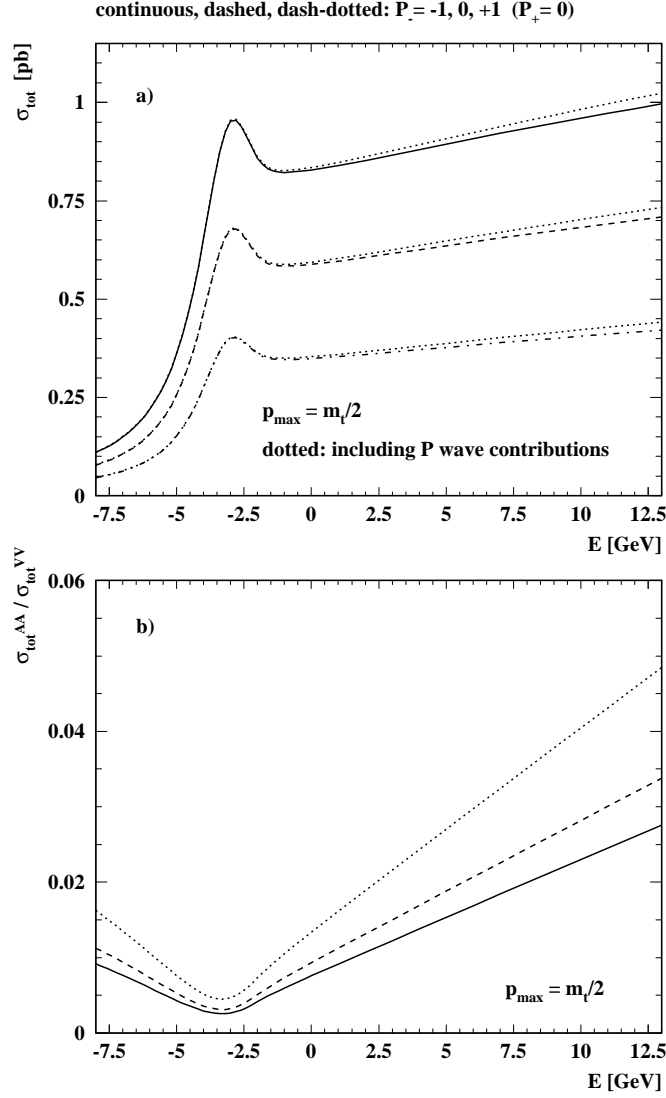


Fig. 8. a) The total cross section $\sigma(e^+e^- \rightarrow t\bar{t})$ as a function of E for three different choices of the e^- polarization: the continuous, dashed and dash-dotted lines correspond to $P_- = -1, 0$ and 1 , respectively, where only S wave production is taken into account. The dotted lines show the corresponding total cross sections including the P wave contributions. b) Ratio of the P to the S wave contribution $\sigma_{\text{tot}}^{\text{AA}} / \sigma_{\text{tot}}^{\text{VV}}$ for the three different e^- polarizations. (Figure taken from [39].)

the so-called potential NRQCD [47], and the dynamics of the $t\bar{t}$ system can

be described by the NNLO Schrödinger equation

$$\left[-\frac{\vec{\nabla}^2}{m_t} - \frac{\vec{\nabla}^4}{4m_t^3} + V_C(\vec{r}) + V_{\text{BF}}(\vec{r}) + V_{\text{NA}}(\vec{r}) - (E + i\Gamma_t) \right] G(\vec{r}, E + i\Gamma_t) = \delta^{(3)}(\vec{r}). \quad (11)$$

Note the appearance of the operator $-\vec{\nabla}^4/(4m_t^3)$ which is a correction to the kinetic energy. The instantaneous potentials are the two-loop corrected Coulomb potential V_C [40], the Breit-Fermi potential V_{BF} known from positronium, and V_{NA} is an additional purely non-Abelian potential. The cross section is again related to the imaginary part of the Green function at $\vec{r} = 0$. In contrast to the NLO calculation the additional potentials lead to ultraviolet divergencies in Eq. (11) which have to be regularized. This can be done by introducing a factorization scale μ_{fac} which serves as a cut-off in the effective field theory. The complete renormalization also requires the matching of the effective field theory to full QCD. This involves the determination of (energy independent) short distance coefficients. They contain all information from the “hard” momenta integrated out before and also depend on the cut-off μ_{fac} , so that in the final result the biggest part of the factorization scale dependence cancels. In order to perform this matching the knowledge of the corresponding NNLO results of the $t\bar{t}$ cross section in full QCD above threshold is essential [48]. Let me skip further details and immediately discuss the results of the NNLO calculation⁷: Fig. 9a shows the total cross section $e^+e^- \rightarrow \gamma^* \rightarrow t\bar{t}$ in units of $\sigma_{\text{point}} = 4\pi\alpha^2/(3s)$ in LO, NLO and NNLO (dotted, dashed and solid lines, respectively), where in each case the three curves correspond to three values of the scale μ_{soft} governing the strong coupling in the potential(s). In Fig. 9b the dependence of the NNLO prediction on the input parameter $\alpha_s(M_Z)$ is demonstrated. These results are somewhat surprising: whereas large corrections are not unusual for NLO calculations, the large corrections arising at NNLO were unexpected. It is well visible from Fig. 9a that from leading to NLO the $1S$ peak is shifted to lower energies by about 1 GeV and again moves by about 300 MeV if one includes the NNLO corrections. Moreover, the large negative correction in the normalization from leading to NLO is partly compensated by the big positive correction at NNLO. In addition the scale uncertainty, which is often used as an estimate of the uncertainty of a (fixed order) perturbative calculation from higher orders, seems to be artificially small at NLO but fairly big again at NNLO. This will make studies which mainly depend on the normalization of the $t\bar{t}$ cross section (like the extraction of the Higgs mass) very difficult.

⁷ A more detailed discussion and complete formulae can be found in [42] (see also [49]).

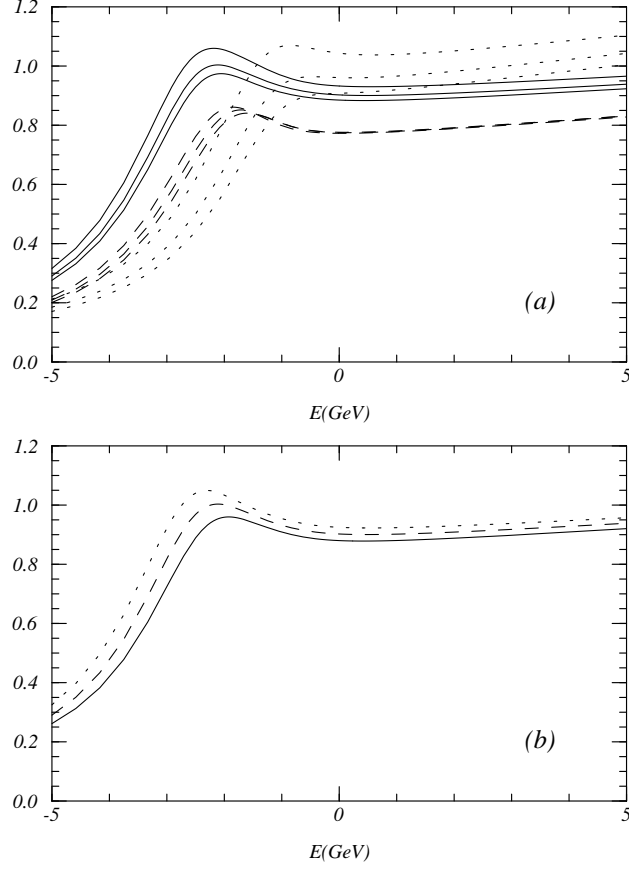


Fig. 9. (a) The total normalized photon-mediated $t\bar{t}$ cross section at LO (dotted lines), NLO (dashed lines) and NNLO (solid lines) for the scales $\mu_{\text{soft}} = 50$ (upper lines), 75 and 100 GeV (lower lines). (b) The NNLO cross section for $\alpha_s(M_Z) = 0.115$ (solid line), 0.118 (dashed line) and 0.121 (dotted line). ($m_t = 175$ GeV, $\Gamma_t = 1.43$ GeV. Figures taken from [42].)

In Fig. 10 the importance of the NNLO relativistic corrections to the kinetic energy and through the additional potentials V_{BF} and V_{NA} in Eq. (11) are demonstrated: the dashed lines show the result where only the NNLO corrections to the static Coulomb potential V_C [40] are applied, the solid lines show the complete NNLO result from [42].

We have argued above that the total cross section with its steep rise in the threshold region (the remainder of the $1S$ peak as shown in Fig. 2) is the “cleanest” observable to determine m_t . From Fig. 9 it now becomes

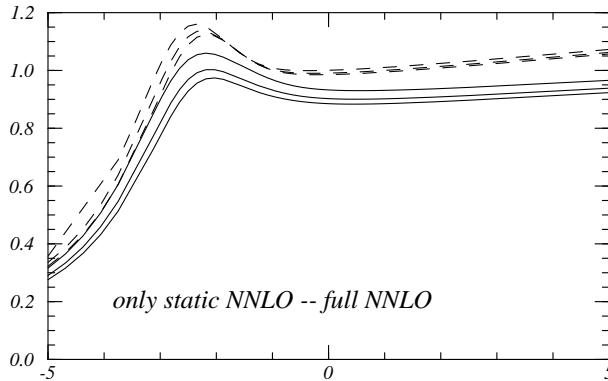


Fig. 10. Total cross section at NNLO as a function of the energy relative to threshold with parameters as in Fig. 9a. The solid lines give the complete result of [42] whereas the dashed lines contain only the NNLO corrections to the static Coulomb potential V_C [40].

clear that the problem of the strong correlation between m_t and α_s , which was already discussed above, also appears through the different orders of perturbation theory: a fit of experimental data from a threshold scan to theoretical predictions (like indicated in Fig. 2) at a given order will result in a determination of m_t depending on the order. This is in principle nothing wrong and is easily understood, as in higher orders the corrections to the potential lead to a stronger effective coupling. Nevertheless now the question arises:

Are there large theoretical uncertainties in the determination of m_t ? First I would like to point out that the $1S$ peak shift from NLO to NNLO is actually not too dramatic. Taking this shift as an estimate of unknown effects in even higher orders would indicate a theoretical uncertainty $\Delta m_t \lesssim \Lambda_{\text{QCD}}$, which still leads to a relative accuracy of $\Delta m_t / m_t \sim \mathcal{O}(10^{-3})$ for the top mass. Still, having argued that due to the large width $\Gamma_t > \Lambda_{\text{QCD}}$ non-perturbative effects should be suppressed, an even smaller theoretical uncertainty should be achievable. Concerning the large NNLO corrections to the normalization and the large scale uncertainty I would like to comment that there is reason to believe that the NNLO result is a much better approximation than the NLO one and that corrections in even higher orders should not spoil this picture [50]. But how can the stability of the prediction be improved? The key point here is to remember that in all formulae and results discussed up to now m_t is defined as the pole mass. This scheme seems, at first glance, to be the most intuitive one and to be suited for the

non-relativistic regime. Nevertheless we know that m^{pole} is *not* an observable. It is defined only up to uncertainties of $\mathcal{O}(\Lambda_{\text{QCD}})$, and the large top quark width Γ_t does not protect the pole mass m_t^{pole} [51]. By performing a renormalon analysis it was recently shown in [52, 53] that the leading long-distance behaviour which affects the pole mass in higher orders also appears in the static potential. However, in the sum $E_{\text{static}} = 2m^{\text{pole}} + E_{\text{binding}}$ these contributions cancel and E_{static} is free from renormalon ambiguities. The separate quantities, mass and potential, suffer from a scheme ambiguity which is not present in the sum. Therefore one should make use of a “short distance” mass definition different from the pole mass scheme, which avoids these large distance ambiguities.

Short distance mass definitions: Curing the problem. In principle there exist infinitely many mass definitions which subtract the renormalon ambiguities. In practice, however, this is not enough. On the one hand, any new short distance mass m^{SD} has to be related with high accuracy to a mass in a more general scheme like the (modified) Minimal Subtraction scheme ($\overline{\text{MS}}$).⁸ Otherwise the extraction of m^{SD} would be more or less useless. On the other hand, the subtraction of renormalon contributions, which become important at high orders of perturbation theory, will not be enough to compensate the large shifts of the $1S$ peak observed at NLO and NNLO. Recently different mass definitions were proposed which can fulfill all the requirements: in Ref. [52] Beneke defined the “Potential Subtracted” mass by

$$m^{\text{PS}}(\mu_f) = m^{\text{pole}} - \delta m(\mu_f) \quad (12)$$

where the subtraction is given by

$$\delta m(\mu_f) = -\frac{1}{2} \int_{|\vec{q}| < \mu_f} \frac{d^3 q}{(2\pi)^3} \tilde{V}(q). \quad (13)$$

The subtracted potential in position space then reads

$$V(r, \mu_f) = V(r) + 2\delta m(\mu_f). \quad (14)$$

This is equivalent to suppressing contributions from momenta q below the scale μ_f in the potential. For $\mu_f \rightarrow 0$ one recovers the pole mass $m^{\text{PS}} \rightarrow m^{\text{pole}}$. By choosing μ_f larger, say 20 GeV, one can achieve a compensation of the $1S$ peak shifts. Another mass definition is the $1S$ mass, originally introduced in B meson physics [54], which defines the $1S$ mass as half of

⁸ This is possible because of the short distance characteristics of m^{SD} and $m^{\overline{\text{MS}}}$ which makes the perturbative relation between the masses well behaved. The $\overline{\text{MS}}$ mass itself cannot be used directly for the calculation of the $t\bar{t}$ threshold, see [52].

the perturbatively defined $1S$ energy. This m^{1S} mass can be related reliably to the $\overline{\text{MS}}$ mass. There are also other mass definition in the literature, see e.g. the “low scale running mass” [55], which is similar to the concept of the PS mass but differs in the actual μ_f -dependent subtraction. Studies about the application of different mass definitions are underway and I can only present preliminary results here: Fig. 11 shows our best prediction [50] for the NNLO $t\bar{t}$ cross section together with the NLO and LO results for two different values of the renormalization scale μ_{soft} governing the strong coupling α_s . In the upper plot the $1S$ mass scheme is used, whereas for the lower plot the PS mass scheme is adopted. It is clear from these curves that both mass definitions work well. The shift of the $1S$ peak is nearly completely compensated. Differences in the normalization remain, but they will not spoil the mass determination from the shape of the total cross section near threshold. Of course more detailed studies are needed to find the best strategy for a precise determination of $m_t^{\overline{\text{MS}}}$, which is needed in electroweak calculations.

3. Studies above Threshold

In the continuum top quarks are produced through the same annihilation process as near threshold: $e^+e^- \rightarrow \gamma^*, Z^* \rightarrow t\bar{t}$. Other (gauge boson fusion) channels like $e^+e^- \rightarrow \nu_e \bar{\nu}_e t\bar{t}$ or $e^+e^- \rightarrow e^+ \bar{\nu}_e t\bar{b}$ are negligible, except for $e^+e^- \rightarrow e^+e^- t\bar{t}$, where the contribution from $\gamma\gamma$ fusion becomes important at TeV energies. Formulae for the (polarized) production cross section and subsequent decay are well known (see e.g. [56] and references therein). Similar to the top quark analyses at Fermilab $t\bar{t}$ events will be reconstructed at an event by event basis and allow for a determination of the top quark mass and its couplings. Due to the clean environment and the large statistics (at $\sqrt{s} = 500$ GeV and with an integrated luminosity of $\int \mathcal{L} = 50 \text{ fb}^{-1}$ there will be $\gtrsim 30000$ $t\bar{t}$ pairs!) high precision will be reached at a future Linear Collider. In the following I will briefly outline a few important cases of top physics above threshold.

- **Kinematical reconstruction of m_t above threshold.** The top can be reconstructed from 6 jet and 4jet+ $l+\nu$ events. For centre of mass energies far above threshold the top and antitop signals will be in different hemispheres and t and \bar{t} may be reconstructed separately. Constraints from energy and momentum conservation in the fitting procedure can improve the mass resolution considerably. Experimental studies [56] (see also [57]) have demonstrated that a high statistical accuracy of the order of $\Delta m_t(\text{stat.}) \sim 150 \text{ MeV}$ can be achieved at a future Linear Collider. But

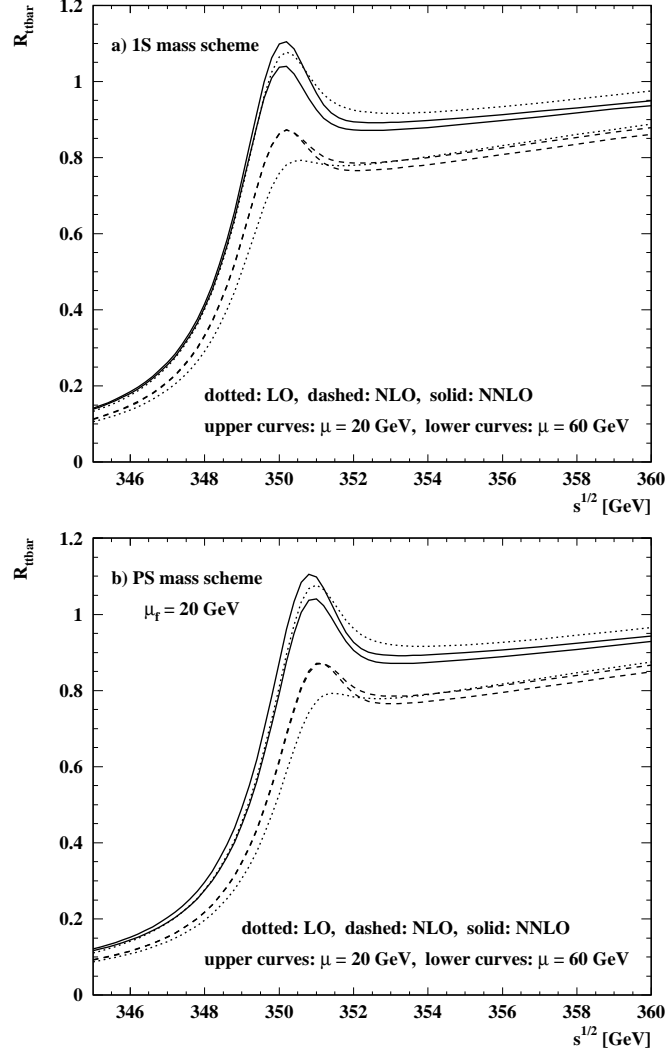


Fig. 11. Total cross section $e^+e^- \rightarrow \gamma^* \rightarrow t\bar{t}$ in units of $\sigma_{\text{point}} = 4\pi\alpha^2/(3s)$ as a function of \sqrt{s} . Dotted, dashed and solid lines correspond to the LO, NLO and NNLO results. The upper curves are obtained with the renormalization scale $\mu = 20$ GeV, the lower ones with $\mu = 60$ GeV. a) 1S mass scheme, and b) PS mass scheme with $\mu_f = 20$ GeV. ($m_t = 175$ GeV, $\Gamma_t = 1.43$ GeV and $\alpha_s(M_Z) = 0.118$.)

in contrast to the analysis at threshold many experimental uncertainties and not very well known hadronization effects will limit the total expected accuracy to $\Delta m_t \sim 0.5$ GeV.

• **Top formfactors.** Top quarks are produced with a high longitudinal polarization. Due to the large top width Γ_t hadronization is suppressed and the initial helicity is transmitted to the final state without depolarization. Therefore, in contrast to the case of light quarks, t helicities can be determined from the (energy-angular) distributions of jets and leptons in the decay $t \rightarrow bW^+ \rightarrow bf\bar{f}'$, similar to the case of Z polarization analyses at LEP and SLC. This will allow to measure the formfactors of the top quark in detail [58]. The relevant current can be written as

$$j_\mu^a \propto \gamma_\mu \left(F_{1,L}^a P_L + F_{1,R}^a P_R \right) + \frac{i\sigma_{\mu\nu} q^\nu}{2m_t} \left(F_{2,L}^a P_L + F_{2,R}^a P_R \right), \quad (15)$$

with the form factors F^a ($a = \gamma, Z, W$). At lowest order in the SM, $F_{1,L}^\gamma = F_{1,R}^\gamma = F_{1,L}^W = 1$, $F_{2,L}^\gamma = F_{2,R}^\gamma = F_{1,R}^W = 0$ and $F_{1,L}^Z = g_L$, $F_{1,R}^Z = g_R$. A non-zero value for $(F_{2,L}^{\gamma,Z} + F_{2,R}^{\gamma,Z})$ is caused by a magnetic (γ) or weak (Z) dipole moment, whereas a non-zero value for the CP-violating combination $(F_{2,L}^{\gamma,Z} - F_{2,R}^{\gamma,Z})$ by an electric (weak) dipole moment. These moments would influence distributions for the top production process, e.g. by inducing an extra contribution proportional to $\sin^2 \theta$ in the differential cross section:

$$\frac{d\sigma}{d\cos\theta} \propto \left[\frac{m_t}{E} (F_{1,L} + F_{1,R}) + \frac{E}{m_t} 2(F_{2,L} + F_{2,R}) \right]^2 \sin^2 \theta. \quad (16)$$

The extra $(F_{2,L} + F_{2,R})$ term leads to an additional spin-flip contribution and therefore changes the total and differential cross section. At a future Linear Collider such an anomalous magnetic moment of the top quark $(g-2)_t$ could be seen up to a limit of $\Delta\delta \lesssim 4\%$ ($\delta \equiv F_{2,L}^\gamma + F_{2,R}^\gamma$) [58], for $\int \mathcal{L} = 50 \text{ fb}^{-1}$ at $\sqrt{s} = 500 \text{ GeV}$. With especially defined observables an anomalous electric and weak dipole moment due to CP violating formfactors $\delta_t^{\gamma,Z} \propto (F_{2,L}^{\gamma,Z} - F_{2,R}^{\gamma,Z})$ could be observed up to a limit of $\Delta d_t^{\gamma,Z} \lesssim 5 \cdot 10^{-18} \text{ ecm}$ (for $\int \mathcal{L} = 10 \text{ fb}^{-1}$ at $\sqrt{s} = 500 \text{ GeV}$).

A measurement of $F_{1,R}^W \neq 0$ would signal non-SM physics like a $(V+A)$ admixture to the top charged current, a W_R boson or the existence of a charged Higgs boson. $F_{1,R}^W$ can be studied by help of the energy and angular distributions of the top quark decay leptons [59]. It could be constrained up to $\Delta\kappa^2 \lesssim 0.02$ ($\kappa^2 \sim |F_{1,R}^W|^2$) with a luminosity of $\int \mathcal{L} = 50 \text{ fb}^{-1}$ in the threshold regime, which is best suited for such a measurement.

• **Rare top decays.** In the SM top quark decays different from $t \rightarrow bW^+$ are strongly suppressed. On one hand, the unitarity of the CKM matrix constrains $V_{tb} \simeq 0.999$, giving not enough room for top decays to the s or d

quark at an observable rate. On the other hand, due to the GIM mechanism [60], flavour-changing one-loop transitions like $t \rightarrow cg$, $t \rightarrow c\gamma$, $t \rightarrow cZ$ or $t \rightarrow cH$ are also extremely small [61, 62]. However, in extensions of the SM like the MSSM extra top quark decay channels like $t \rightarrow bH^+$, $t \rightarrow \tilde{t}\tilde{\chi}^0$, $\tilde{b}\tilde{\chi}_1^+$ may be open. In general branching fractions of up to 30% are possible. The experimental signatures are clear and will be easily detectable [63, 3]. With an integrated luminosity of $\int \mathcal{L} = 50 \text{ fb}^{-1}$ it will be possible to observe $t \rightarrow bH^+$ up to $m_{H^+} \lesssim m_t - 15 \text{ GeV}$, and $t \rightarrow \tilde{t}\tilde{\chi}^0$ down to a branching fraction of $\sim 1\%$ at the 3σ level.

• **Direct observation of the top Yukawa coupling.** Although the Higgs boson will hopefully be discovered before the future Linear Collider starts operation, the detailed study of the Higgs and its couplings will remain one of the main tasks of the LC. There one will be able to test if the Higgs Yukawa coupling to the top quark deviates from the SM value $\lambda_t^2 = \sqrt{2} G_F m_t^2 \sim 0.5$. Studies at threshold will be difficult (see above), but due to this large coupling (in comparison to $\lambda_b^2 \sim 4 \cdot 10^{-4}$) the $t\bar{t}H^0$ vertex will be accessible through Higgs-strahlung at high energies. For $M_H \leq 2m_t$ one will measure λ_t^2 through the process $e^+e^- \rightarrow t\bar{t}H$ with the Higgs subsequently decaying into a pair of b quarks. For $M_H \geq 2m_t$ two different processes will be dominant: Higgs radiation from Z (in $e^+e^- \rightarrow ZH$) with subsequent decay of the Higgs into $t\bar{t}$, and the fusion of W^+W^- (in $e^+e^- \rightarrow \nu\bar{\nu}H$) into the Higgs which then decays into $t\bar{t}$. With eight jets in the final state of the fully hadronic decay channels, which satisfy many constraints, these processes will have clear signatures. Still, even despite the large Yukawa coupling, the cross sections are quite small, amounting only to a few fb. Here the planned high luminosity of the latest TESLA design will be most welcome. Extensive studies were performed and come to the conclusion that at high energy and with high luminosity λ_t^2 may finally be measurable with an accuracy of 5% at a future LC [64].

4. Conclusions

I have reviewed the subject of top quark physics at a future e^+e^- Linear Collider, emphasizing top quark physics at threshold. Threshold studies will determine the SM parameters m_t , α_s and Γ_t with very high accuracy: $\Delta m_t/m_t \lesssim 10^{-3}$, $\Delta\alpha_s \lesssim 0.003$ and $\Delta\Gamma_t/\Gamma_t \lesssim 0.05$ seem to be possible from experimental point of view. Recent theoretical progress shows, that in order to achieve such a high accuracy also in the theoretical predictions, mass schemes different from the pole mass should be employed to disentangle

gle correlations between m_t and α_s as well as infrared ambiguities in the definition of m_t^{pole} .

In addition to the total cross section and the momentum distribution of top quarks also observables like the forward-backward asymmetry, polarization and axial contributions are calculated. These observables will be accessible by help of large statistics due to the high luminosity and by the possibility to have polarized e^+e^- beams. Above threshold formfactors of the top quark and the top Yukawa coupling will be measured. One may study rare top decays and get sensitive to non-SM physics.

The future Linear Collider will therefore be *the* machine to study top quark physics in detail, to understand the SM better and eventually to learn more about what comes beyond it. I hope to have shown that top quark physics is an interesting field both for Theory and Experiment. Further work will be needed to understand the heaviest known particle better, before data become available.

Acknowledgements

It is my great pleasure to thank the organizers for having made the *Cracow Epiphany Conference '99* such an enjoyable and stimulating event. I would also like to express my gratitude to all friends and colleagues I have worked with on various topics about toppik and top peaks reported here for their fruitful collaboration.

While writing this contribution I was hit by the shock of the tragic death of Bjørn H. Wiik. His outstanding efforts for the future Linear Collider and his fascinating personality will be missed.

REFERENCES

- [1] J.H. Kühn, *Acta Phys. Polon.* **B 12** (1981) 347; *Act. Phys. Austr.* Suppl. XXIV (1982) 203.
I.Y. Bigi, Yu.L. Dokshitzer, V.A. Khoze, J.H. Kühn, and P.M. Zerwas, *Phys. Lett.* **B 181** (1986) 157.
- [2] R. Brinkmann et al. (Eds.), *Conceptual Design of a 500 GeV e^+e^- Linear Collider with Integrated X-ray Laser Facility*, DESY Orange Preprint DESY 1997-048 and ECFA 1997-182.
- [3] E. Accomando et al., *Phys. Rep.* **299** (1998) 1.
- [4] I.I. Bigi, F. Gabbiani and V.A. Khoze, *Nucl. Phys.* **B 406** (1993) 3.
O.J.P. Eboli, M.C. Gonzalez-Garcia, F. Halzen, and S.F. Novaes, *Phys. Rev.* **D 47** (1993) 1889.
J.H. Kühn, E. Mirkes and J. Steegborn, *Z. Phys.* **C 57** (1993) 615.

- [5] J.H. Kühn, University of Karlsruhe Preprint TTP-96-18 and **hep-ph/9707321**, published in the proceedings of the *23rd SLAC Summer Institute, Stanford, CA, 10-21 July 1995*, SLAC Report 494.
- [6] V.A. Khoze, W.J. Stirling and L.H. Orr, *Nucl. Phys.* **B 378** (1992) 413.
L.H. Orr, T. Stelzer and W.J. Stirling, *Phys. Lett.* **B 354** (1995) 442.
C. Maccesanu and L.H. Orr, Rochester U. Preprint, UR-1542 and **hep-ph/9808403**.
- [7] V.S. Fadin and V.A. Khoze, *Z. Phys.* **C 46** (1987) 417 [*JETP Lett.* **46** (1987) 525]; *Yad. Fiz.* **48** (1988) 487 [*Sov. J. Nucl. Phys.* **48** (1988) 309].
- [8] CDF Collaboration (F. Abe, et al.), *Phys. Rev. Lett.* **82** (1999) 271.
- [9] D0 Collaboration (B. Abbott, et al.), FERMILAB-PUB-98-261-E and **hep-ex/9808029**.
- [10] A. Juste, M. Martinez and D. Schulte, in *e^+e^- Linear Colliders: Physics and Detector Studies*, DESY Orange Report 97-123E;
P. Comas, R. Miquel, M. Martinez, and S. Orteu, in *e^+e^- at TeV Energies: The Physics Potential*, DESY Orange Report 96-123D;
P. Igo-Kemenes, M. Martinez, R. Miquel, and S. Orteu, in *e^+e^- at 500 GeV: The Physics Potential*, DESY Orange Report 93-123C.
- [11] K. Fujii, T. Matsui and Y. Sumino, *Phys. Rev.* **D 50** (1994) 4341.
- [12] M. Jeżabek, *Nucl. Phys. Proc. Suppl.* **B37** (1994) 197.
- [13] M. Jeżabek and J.H. Kühn, *Phys. Lett.* **B 207** (1988) 91.
- [14] A. Denner and T. Sack, *Nucl. Phys.* **B 358** (1991) 46.
R. Migneron, G. Eilam, R.R. Mendel, and A. Soni, *Phys. Rev. Lett.* **66** (1991) 3105.
- [15] M. Jeżabek and J.H. Kühn, *Phys. Rev.* **D 48** (1993) 1910; *Phys. Rev.* **D 49** (1994) 4970 (E).
- [16] A. Czarnecki and K. Melnikov, BNL-HET-98-21 and **hep-ph/9806244**.
- [17] R. Harlander, M. Jeżabek and J.H. Kühn, *Acta Phys. Polon.* **B 27** (1996) 1781, and references therein.
- [18] W. Kwong, *Phys. Rev.* **D 43** (1991) 1488.
- [19] M.J. Strassler and M.E. Peskin, *Phys. Rev.* **D 43** (1991) 1500.
- [20] Y. Sumino, K. Fujii, K. Hagiwara, H. Murayama, and C.K. Ng, *Phys. Rev.* **D 47** (1993) 56.
- [21] M. Jeżabek, J.H. Kühn and T. Teubner, *Z. Phys.* **C 56** (1992) 653.
- [22] W. Fischler, *Nucl. Phys.* **B 129** (1977) 157.
A. Billoire, *Phys. Lett.* **B 92** (1980) 343.
- [23] R. Barbieri, R. Kögerler, Z. Kunszt, and R. Gatto, *Nucl. Phys.* **B 105** (1976) 125.
- [24] H. Murayama and Y. Sumino, *Phys. Rev.* **D 47** (1993) 82.

- [25] R. Harlander, M. Jeřabek, J.H. Kühn, and T. Teubner, *Phys. Lett. B* **346** (1995) 137.
- [26] M. Jeřabek and T. Teubner, *Z. Phys. C* **59** (1993) 669.
- [27] W. Mödritsch and W. Kummer, *Nucl. Phys. B* **430** (1994) 3.
- [28] V.S. Fadin, V.A. Khoze and A.D. Martin, *Phys. Lett. B* **320** (1994) 141; *Phys. Rev. D* **49** (1994) 2247.
- [29] K. Melnikov and O. Yakovlev, *Phys. Lett. B* **324** (1994) 217; *Nucl. Phys. B* **471** (1996) 90.
- [30] V.A. Khoze, CERN Preprint CERN-TH-98-176 and hep-ph/9805505.
- [31] R. Harlander, M. Jeřabek, J.H. Kühn, and M. Peter, *Z. Phys. C* **73** (1997) 477.
- [32] M. Peter and Y. Sumino, *Phys. Rev. D* **57** (1998) 6912.
- [33] R.J. Guth and J.H. Kühn, *Nucl. Phys. B* **368** (1992) 38.
- [34] W. Beenakker and W. Hollik, *Phys. Lett. B* **269** (1991) 425.
W. Beenakker, S.C. van der Marck and W. Hollik, *Nucl. Phys. B* **365** (1991) 24.
- [35] W. Hollik and C. Schappacher, University of Karlsruhe Preprint KA-TP-3-1998 and hep-ph/9807427, *Nucl. Phys. B* (in press).
- [36] V.S. Fadin, V.A. Khoze and M.I. Kotskii, *Z. Phys. C* **64** (1994) 45.
- [37] M. Peter, *Acta Phys. Polon. B* **27** (1996) 3805.
- [38] Y. Sumino, *Acta Phys. Polon. B* **28** (1997) 2461.
Y. Sumino and M. Jeřabek, *Acta Phys. Polon. B* **29** (1998) 1443.
- [39] J.H. Kühn and T. Teubner, DESY Orange Preprint DESY-99-031 and hep-ph/9903322, *Eur. Phys. J. C* (in press).
- [40] M. Peter, *Nucl. Phys. B* **501** (1997) 471; *Phys. Rev. Lett.* **78** (1997) 602.
Y. Schröder, *Phys. Lett. B* **447** (1999) 321.
- [41] M. Jeřabek, J.H. Kühn, M. Peter, Y. Sumino, and T. Teubner, *Phys. Rev. D* **58** (1998) 14006.
M. Jeřabek, M. Peter and Y. Sumino, *Phys. Lett. B* **428** (1998) 352.
- [42] A.H. Hoang and T. Teubner, *Phys. Rev. D* **58** (1998) 114023.
- [43] K. Melnikov and A. Yelkhovskii, *Nucl. Phys. B* **528** (1998) 59.
- [44] O. Yakovlev, University of Würzburg Preprint WUE-ITP-98-036 and hep-ph/9808463.
- [45] M. Beneke, A. Signer and V.A. Smirnov, CERN Preprint CERN-TH-99-57 and hep-ph/9903260.
- [46] W.E. Caswell and G.E. Lepage, *Phys. Lett. B* **167** (1986) 437.
G.T. Bodwin, E. Braaten and G.P. Lepage, *Phys. Rev. D* **51** (1995) 1125; *Phys. Rev. D* **55** (1997) 5853 (Erratum).
- [47] A. Pineda and J. Soto, *Nucl. Phys. Proc. Suppl. B* **64** (1998) 428.

- [48] A. Czarnecki and K. Melnikov, *Phys. Rev. Lett.* **80** (1998) 2531, and references therein.
- [49] A.H. Hoang, *Phys. Rev. D* **59** (1999) 14039.
A.H. Hoang, University of California, San Diego, Preprint UCSD-PTH-98-33 and [hep-ph/9809431](#).
- [50] A.H. Hoang and T. Teubner, in preparation.
- [51] M. Beneke and V.M. Braun, *Nucl. Phys. B* **426** (1994) 301.
I.I. Bigi, M.A. Shifman, N.G. Uraltsev, and A.I. Vainshtein, *Phys. Rev. D* **50** (1994) 2234.
M. Beneke, *Phys. Lett. B* **344** (1995) 341.
M.C. Smith, S. Willenbrock, *Phys. Rev. Lett.* **79** (1997) 3825.
- [52] M. Beneke, *Phys. Lett. B* **434** (1998) 115.
- [53] A.H. Hoang, M.C. Smith, T. Stelzer, and S. Willenbrock, University of California, San Diego, Preprint UCSD-PTH-98-13 and [hep-ph/9804227](#).
- [54] A.H. Hoang, Z. Ligeti and A.V. Manohar, *Phys. Rev. Lett.* **82** (1999) 277; *Phys. Rev. D* **59** (1999) 74017.
- [55] M.B. Voloshin, *Phys. Rev. D* **46** (1992) 3062.
I. Bigi, M. Shifman, N. Uraltsev, and A. Vainshtein, *Phys. Rev. D* **56** (1997) 4017.
A. Czarnecki, K. Melnikov and N. Uraltsev, *Phys. Rev. Lett.* **80** (1998) 3189.
- [56] P.M. Zerwas (Ed.), *e^+e^- Collisions at 500 GeV: The Physics Potential*, Part A, DESY Orange Report DESY92-123A.
- [57] E. Accomando, A. Ballestrero and M. Pizzio, in *e^+e^- Linear Colliders: Physics and Detector Studies*, DESY Orange Report 97-123E.
- [58] M. Schmitt, in *e^+e^- at TeV Energies: The Physics Potential*, DESY Orange Report 96-123D.
- [59] M. Jezabek and J.H. Kühn, *Phys. Lett. B* **329** (1994) 317; *Nucl. Phys. B* **320** (1989) 20.
M. Jezabek, *Acta Phys. Polon. B* **26** (1995) 789.
- [60] S.L. Glashow, J. Iliopoulos and L. Maiani, *Phys. Rev. D* **2** (1970) 1285.
- [61] G. Eilam, B. Haeri and A. Soni, *Phys. Rev. D* **41** (1990) 875.
- [62] B. Mele, S. Petrarca and A. Soddu, *Phys. Lett. B* **435** (1998) 401.
- [63] A. Venturi, in *e^+e^- at 500 GeV: The Physics Potential*, DESY Orange Report 93-123C.
B. Bagliesi et al., in Ref. [56].
- [64] T. Matsui, contribution to these proceedings.
M. Martinez and S. Orteu, in *e^+e^- at TeV Energies: The Physics Potential*, DESY Orange Report 96-123D.
A. Juste and G. Merino; M. Sachwitz, S. Shichanin and H.J. Schreiber, talks presented at the *2nd ECFA/DESY Study for Physics and Detectors for a Linear Collider*, 7-10 November 1998, Frascati, Italy. To appear in the proceedings.